Three-Phase Equilibria Using Equations of State

It is demonstrated that a single equation of state may be used to describe all three phases in liquid-liquid-vapor equilibrium situations. Wilson's version of the Redlich-Kwong equation is shown to predict accurately the water solubility in normal paraffins with interaction parameters $k_{12} = 0.50$. A simple procedure for three-phase flash computations is presented. Results obtained using this procedure for the system methane, *n*-butane, water exhibit many of the characteristics of the experimental data of McKetta and Katz (1948). In particular, the water content of the vapor phase and the liquid hydrocarbon phase are accurately predicted.

ROBERT A. HEIDEMANN

Department of Chemical Engineering
University of Calgary
Calgary, Alberta T2N 1N4, Canada

SCOPE

Equations of state, such as the Benedict-Webb-Rubin equation and the Redlich-Kwong equation, have been increasingly used to describe both phases in vapor-liquid equilibrium computations. In this paper it is shown that it is possible to perform three-phase liquid-liquid-vapor computations using the same equation of state to describe all three phases.

Three-phase equilibria occur in the production and processing of natural gas and petroleum wherever significant amounts of water are present. At cryogenic temperatures and high pressures, systems such as methane, *n*-heptane (Kohn, 1961) and nitrogen, propane (Schindler et al., 1966) have been reported to show liquid miscibility gaps.

Although this paper is limited to water, normal paraffin examples and only Wilson's version of the Redlich-Kwong equation is considered, the general approach taken is applicable to other equations of state and to other kinds of mixtures. The ability of an equation of state to predict liquid immiscibility and quantitatively correct solubility data provides yet another criterion for evaluation.

The computational problems in three-phase equilibria are not trivial. A new algorithm is proposed here for three-phase flash calculations.

CONCLUSIONS AND SIGNIFICANCE

It has been demonstrated that the liquid phase described by Wilson's version of the Redlich-Kwong equation can be unstable and can separate into two liquid phases of different compositions at equilibrium, depending on the values of the binary interaction parameters. A value of $k_{12} = 0.50$ for normal paraffin, water pairs is found to predict the water solubility in the hydrocarbon liquid with reasonable accuracy. These results open the possibility of using a single equation of state to describe all three phases in liquid-liquid-vapor equilibrium computations.

A new computation scheme for multiphase flash problems was presented. This scheme, which is based on free energy minimization, is reliable and easily programmed and may be extended to equilibrium computations with more than three phases present.

Using the new computational scheme, it was possible to show that Wilson's version of the Redlich-Kwong equation predicts phase behavior in three-phase systems which exhibit many of the characteristics of experimental systems. In a detailed study of the system methane, *n*-butane, water it was found that the water content of both the liquid hydrocarbon and the vapor phase were predicted with satisfactory precision for design purposes. Liquid-liquid equilibria computed at pressures above the three-phase critical pressure also agree with the available experimental data.

The general approach used in this paper of describing all three phases by the same equation of state in three-phase equilibrium situations can be applied to equations other than Wilson's version of the Redlich-Kwong equation.

WILSON'S REDLICH-KWONG EQUATION

The version of the Redlich-Kwong equation which is used in this paper was proposed by Wilson (1969). It includes some modifications of equations proposed earlier by Wilson (1964), (1966).

The equation is

$$P = \frac{RT}{V - b} - \frac{RT\,a}{V(V + b)} \qquad (1)$$

where

$$b = \Sigma\, x_i\, b_i \qquad (2)$$

and

$$a = \Sigma\Sigma\, x_i\, x_j\, a_{ij} \qquad (3)$$

The pure component coefficients b_i are found in the usual way

$$b_i = 0.0865\, RT_{ci}/P_{ci} \qquad (4)$$

Coefficients a_{ij} are temperature dependent in a way which

is intended, in part, to match pure component vapor pressure data. The equation is

$$a_{ij} = 2.467\, b_i \left(\frac{T_{cj}\, k_{ij}}{T}\right)^{0.12} \left[1 + (1.45 + 1.62\omega_j)\left(\frac{T_{cj}\, k_{ij}}{T} - 1\right)\right] + 2.467\, b_j \left(\frac{T_{ci}\, k_{ij}}{T}\right)^{0.12} \left[1 + (1.45 + 1.62\omega_i)\left(\frac{T_{ci}\, k_{ij}}{T} - 1\right)\right] \quad (5)$$

Coefficient k_{ij} is the so-called "interaction parameter" and must be obtained by fitting binary data. For pure components,

$$k_{ii} = 1 \quad (6)$$

Wilson (1969) has reported comparisons between experimental vapor-liquid equilibria data and equilibria computed using the above equations to describe both the vapor and the liquid phase. In many cases the match of experimental data is very good.

Equation (1) is taken to apply to both the liquid and the vapor phase. At a given temperature and pressure, Equation (1) is satisfied by as many as three real positive values for the molar volume V. It is conventional to take the smallest and the largest positive values to represent the volume of potential liquid and vapor phases, respectively. Then the fugacity of component i in the phase having volume V is given by

$$\ln f_i = \ln [x_i RT/(V-b)] + (Z-1)b_i/b + [b_i \sum_j \sum_k x_j\, x_k\, a_{jk}/b^2 - 2 \sum_j x_j\, a_{ij}/b] \cdot \ln [(V+b)/V] \quad (7)$$

The necessary criteria for equilibrium between two phases, phase I and phase II, are satisfied if, for each component of the phases,

$$f_{iI} = f_{iII} \quad (8)$$

Any computational procedure for phase equilibria using equations of state rests, in the end, on finding phase compositions for which Equation (8) is satisfied.

LIQUID INSTABILITY

It happens that the liquid phase described by Equations (1) through (7), when V is taken to be the smallest positive value which satisfies Equation (1), can be unstable. That is, at equilibrium, the liquid must separate into two phases having different compositions.

That this is true may be seen by looking at the Gibbs free energy of mixing curve for the liquid phase. The textbook treatment of liquid immiscibility is usually presented with the use of such curves. [See for instance, Prausnitz (1969)].

Taking the standard state to be the pure components at unit fugacity and at the given temperature, the standard free energy of mixing for a binary system is given by

$$\Delta G^M/RT = x_1 \ln f_1 + x_2 \ln f_2 \quad (9)$$

Fugacities f_1 and f_2 must be in atmospheres in this expression. At a given temperature and pressure, $\Delta G^M/RT$ is a function of mole fraction x_1 alone. The curve of $\Delta G^M/RT$ versus x_1 is tangent to the vertical at both $x_1 = 0$ and at $x_1 = 1$. At $x_1 = 0^+$, the derivative is $-\infty$ and at $x_1 = 1^-$ the derivative is $+\infty$.

Figure 1 presents free energy of mixing curves for *n*-butane and water at 289°K (60°F) and 6.8 atm (100 lb./sq.in.) with various values of the interaction parameter k_{12}. This figure has been constructed using Wilson's version of the Redlich-Kwong equation with fugacities as given by Equation (7). The curves must indeed be tangent to the vertical at $x_1 = 0^+$ and $x_1 = 1^-$, approaching from below. Because the change in curvature takes place on such a small scale near the axes it is impossible to show this behavior in the figure.

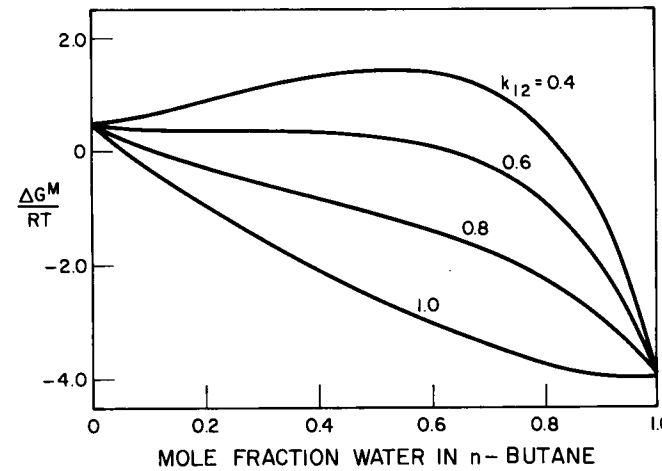

Fig. 1. Standard free energy of mixing for water, *n*-butane at 289°K for various interaction parameters.

TABLE 1. EFFECT OF THE INTERACTION PARAMETER ON CALCULATED MUTUAL SOLUBILITIES OF LIQUID *n*-BUTANE AND WATER AT 289°K

Interaction parameter	Mole fraction *n*-butane in water	Mole fraction water in *n*-butane
0.92	0.00768	0.4603
0.90	0.001738	0.2911
0.80	1.42×10^{-6}	0.04224
0.70	1.175×10^{-9}	0.007717
0.60	1.108×10^{-11}	1.514×10^{-3}
0.50	1.256×10^{-15}	3.040×10^{-4}
0.40	—	6.846×10^{-5}

According to arguments first presented by Gibbs, if a line can be drawn tangent to the free energy of mixing curve at two points, any mixture of composition between the two points of tangency must, at equilibrium, separate into two phases which have the end point compositions.

In Figure 1, it is possible to draw such a tangent line to each of the curves except for $k_{12} = 1.0$. That is, liquid *n*-butane, water mixtures at 289°K, 6.8 atm are predicted to separate into two phases for interaction parameters less than some value between 0.8 and 1.0. The composition of the two phases can, in theory, be determined from the points of tangency of a common tangent line. For the water rich phase at least, this composition is apparently very close to being a pure phase.

Using a computational procedure which is described in detail in Appendix, the predicted mutual solubilities for *n*-butane and water have been calculated for various values of k_{12}. These results appear in Table 1.

The predicted solubility of *n*-butane in water is consistently many orders of magnitude lower than the solubility of water in *n*-butane. It proves impossible to select a single value of the interaction parameter which predicts both mutual solubilities adequately. It was decided to concentrate on matching the data for the hydrocarbon-rich

Table 2. Interaction Parameters for Water-Hydrocarbon Systems at 289°K

	Interaction parameter
Propane	0.46
n-butane	0.452
n-pentane	0.475
n-hexane	0.502
n-heptane	0.502
n-octane	0.502

Table 3. Calculated Solubility of *n*-Butane in H_2O

T°K	$k_{12} = 0.45$ mole fraction water	$k_{12} = 0.5$ in n-butane	Experimental
289	1.401×10^{-4}	3.04×10^{-4}	1.5×10^{-4}
311	3.83×10^{-4}	7.60×10^{-4}	4.7×10^{-4}
339	1.156×10^{-3}	2.08×10^{-3}	1.75×10^{-3}
367	3.140×10^{-3}	5.160×10^{-3}	5.4×10^{-3}
394	8.387×10^{-3}	1.256×10^{-2}	1.5×10^{-2}

phase in this work.

The data of Table 1 plot as a straight line on semi-logarithmic paper with k_{12} on the linear axis. This fact permits interpolation to find the value of k_{12} which matches the experimental data. Data for the solubility of water in hydrocarbons are available in the API Technical Data Book (1970). In Table 2 are tabulated values of the interaction parameter for water and selected normal paraffins which permit Wilson's version of the Redlich-Kwong equation to predict the experimental solubility of water in the hydrocarbon.

TEMPERATURE VARIATION OF WATER SOLUBILITY

Calculations were performed for the predicted mutual solubilities of water and *n*-butane over a range of temperatures with $k_{12} = 0.45$ and $k_{12} = 0.50$. The results of these computations appear in Table 3.

It is clear that the calculated solubilities show the correct qualitative behavior, increasing exponentially with temperature. It is also clear that quantitatively accurate solubilities of water in *n*-butane cannot be obtained with a single constant value of k_{12}.

Based on the computed results of Tables 2 and 3 it was decided to recommend that a constant value $k_{12} = 0.50$ be used for water and normal paraffins. There will undoubtedly be some loss in accuracy of calculated solubilities at higher temperatures. Considering, however, that the predicted solubility of hydrocarbons in the water layer is low by many orders of magnitude it appears inconsistent to add the complexity of making k_{12} a temperature function. A value of $k_{12} = 0.50$ permits reasonably accurate solubility predictions for water in *n*-butane over a temperature range from 300° to 400°K.

LIQUID-LIQUID-VAPOR EQUILIBRIA

If three phases are present in a system at equilibrium it is necessary for each component which is present in all three phases, that

$$f_{iI} = f_{iII} = f_{iIII} \tag{10}$$

This equation follows from the requirement that the Gibbs free energy be a minimum.

Free energy of mixing curves can be of value in determining equilibrium conditions even in liquid-vapor or liquid-liquid-vapor systems. On solving Equation (1) for

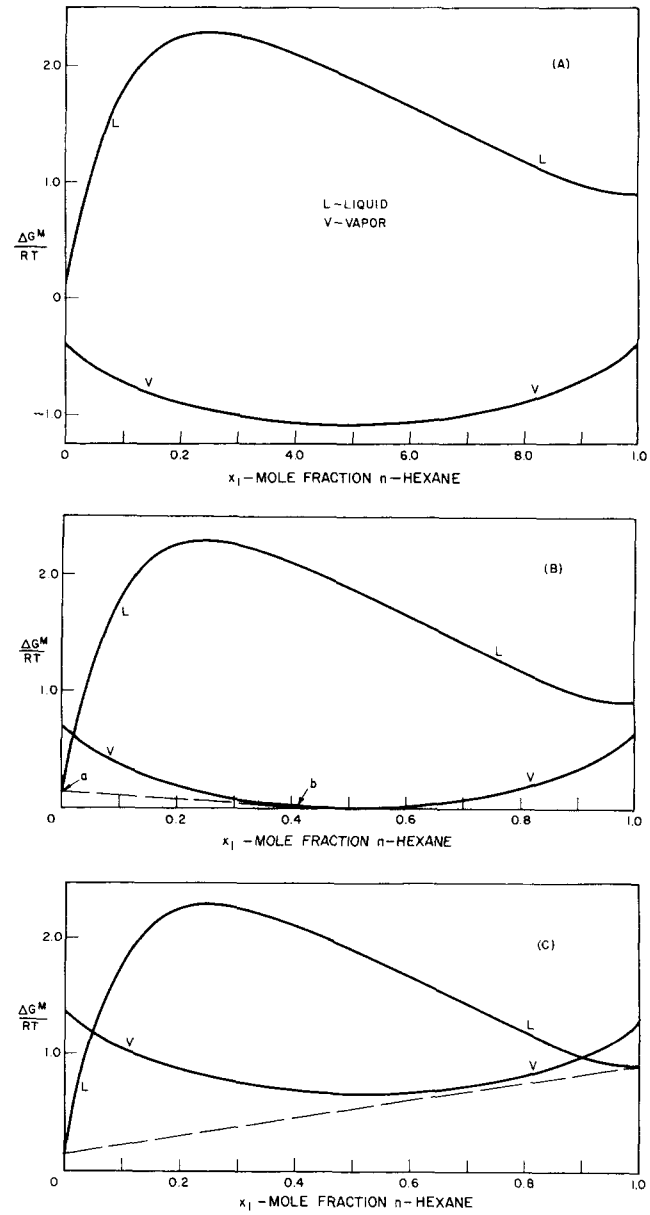

Fig. 2. Standard free energy of mixing for water, *n*-hexane at 378°K and various pressures. (A) P = 0.68 atm, (B) P = 2.04 atm, (C) P = 4.08 atm.

V at a given temperature and pressure for a binary mixture, it is possible to prepare a free energy of mixing curve for the vapor phase as well as for the liquid phase by using the largest positive value of V as the volume of the vapor. By inspection of these two curves it is then possible to decide whether, for a given binary composition, the condition of minimum Gibbs free energy is met when the system is homogeneous in the liquid or in the vapor phase or whether the system must separate into two phases.

The necessary condition of equilibrium between two phases is met if the free energy of mixing curves have a common tangent line, just as in the liquid-liquid equilibrium case.

Figures 2 and 3 present free energy of mixing curves and their evolution with pressure for *n*-hexane and water at 378°K (220°F) and 450°K (350°F), respectively, with $k_{12} = 0.5$. Figure 2 is somewhat more simple than Figure 3. At each of the pressures considered in Figure 2 and over the whole composition range, the equation of state is satisfied by three volumes.

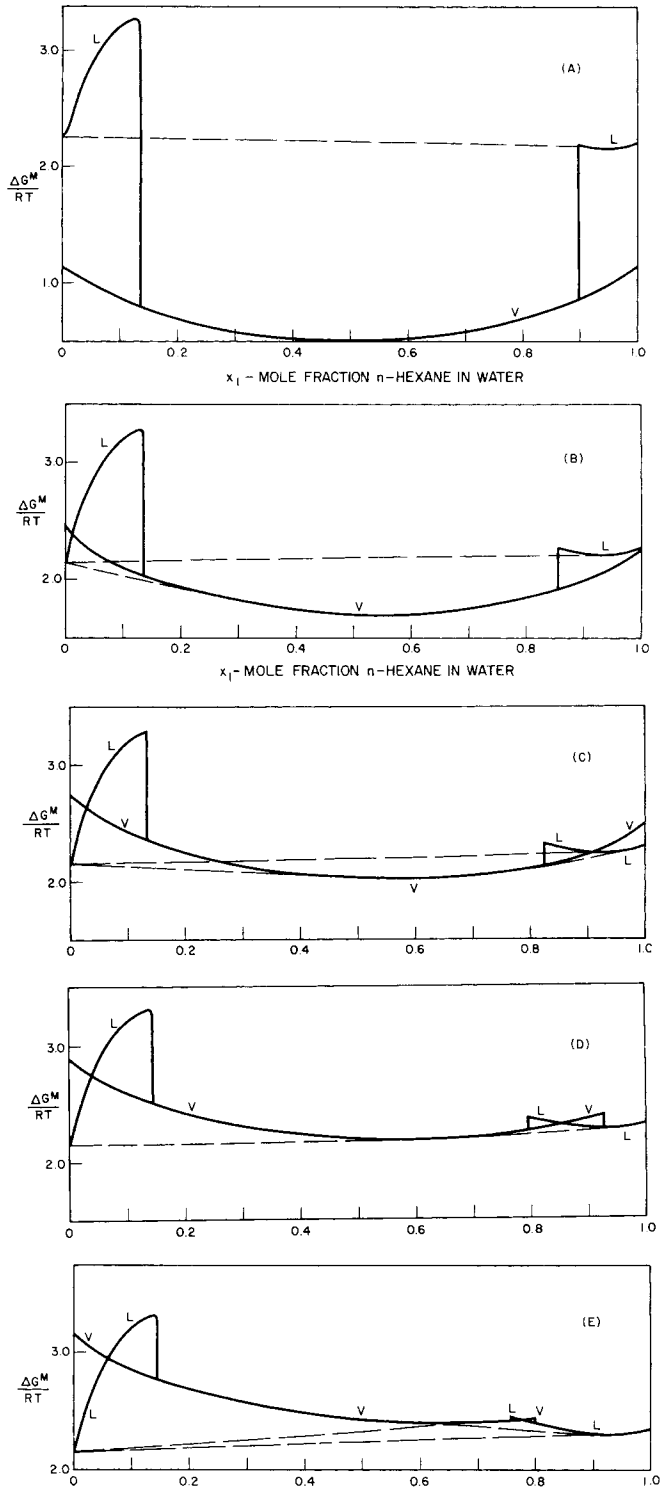

Fig. 3. Standard free energy of mixing for water, *n*- hexane at 450°K and various pressures. (A) P = 3.40 atm, (B) P = 5.10 atm, (C) P = 17.0 atm, (D) P = 20.4 atm, (E) P = 27.2 atm.

In Figure 2a, where $P = 0.68$ atm (10 lb./sq.in.), the vapor free energy of mixing curve lies completely below the liquid curve. The homogeneous vapor therefore has the minimum possible Gibbs free energy, regardless of composition.

At 2.04 atm (30 lb./sq.in.), the condition of Figure 2b, the vapor pressure of water is exceeded. Over a composition range, whose endpoints are indicated by points *a* and *b*, the system must divide into a liquid phase, which is almost pure water, and a vapor phase. The free energy of mixing curves have a common tangent line with points of tangency at points *a* and *b*, respectively. If the mole fraction of *n*-hexane exceeds that at point *b* the mixture remains a homogenous vapor.

In Figure 2c the pressure is 4.08 atm (60 lb./sq.in.) and is well above the vapor pressure of *n*-hexane. It can be seen that a tangent line can be drawn between two points on the liquid curve, representing almost pure water and almost pure hexane, which line lies completely below both the vapor and liquid curves. At some pressure, just below 4.08 atm, this line would be tangent to the vapor curve as well. At 4.08 atm, two liquid phases must be at equilibrium. At some specific pressure just below 4.08 atm it would be possible to have two liquid phases and a vapor phase at equilibrium.

Figure 3, in which the temperature is 450°K, shows the same qualitative behavior as pressure is increased. From Figure 3a, at $P = 3.40$ atm (50 lb./sq.in.), we conclude that any mixture of *n*-hexane and water is wholly in the vapor phase at equilibrium. At 5.10 atm (75 lb./sq.in.) there is one region of vapor-liquid equilibrium. At pressures of 17.0 and 20.4 atm (250 and 300 lb./sq.in.) there are two separate regions of vapor-liquid equilibrium. When the conditions of Figure 3e are reached, with $P = 27.2$ atm (400 lb./sq.in.), there can be no vapor phase and, over a broad range of compositions, mixtures of *n*-hexane and water must separate into two liquid phases.

The new feature of Figure 3 is that the free energy of mixing curves for both the liquid and vapor phases are shown to have discontinuities. These discontinuities occur when, at some composition, the equation of state changes from having three volume roots to having only one root. It is possible that either the largest or smallest positive volume becomes discontinuous with composition.

In principle these features can be dealt with without ambiguity and correct conclusions can be drawn regarding conditions at equilibrium. It must be apparent, however, that certain computational problems can occur. The disappearance of a root to the equation of state corresponding to a liquid volume could cause an iterative procedure to fail. These difficulties, however, are not peculiar only to liquid-liquid-vapor computations.

There are some additional problems possible which become apparent on inspection of Figure 3e. In addition to the line tangent to the liquid curve at two points in this figure, it is possible to draw two lines each of which is tangent to both the liquid curve and the vapor curve. On each of these lines, the points of tangency obey the necessary conditions for vapor-liquid equilibrium; that is, equality of fugacities. If a mixture containing 0.65 mole fraction *n*-hexane in water is flashed it will be seen from Figure 3e that it is possible to compute two different pairs of vapor-liquid phase compositions at which Equation (8) is satisfied for both components. Neither composition pair will be correct since the correct equilibrium condition has two liquid phases.

COMPUTATIONAL SCHEME

In performing the three-phase and liquid-liquid equilibrium computations in this work, we used a new calculation procedure which, it is believed, avoids some of the potential difficulties outlined above.

Erbar (1973) has outlined a computational scheme for three-phase equilibrium problems. His formulation of the problem is similar to that of Deam and Maddox (1969). It involves evaluating phase equilibrium constants K_i and proceeds in an iterative manner until the sum of the mole fractions in all phases is one. Erbar has reported results of computations for a hydrocarbon, water liquid-liquid-vapor system and for solid-liquid-vapor systems in which

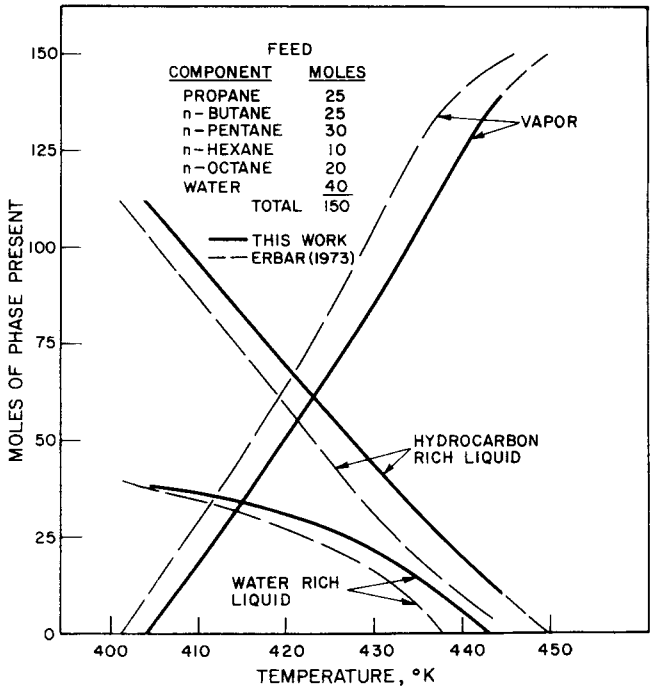

Fig. 4. Condensation curves predicted for a hydrocarbon-water mixture at 23.8 atm.

TABLE 4. THREE-PHASE FLASH RESULTS

$T = 422°K, (300°F)$ $P = 23.8$ atm, (350 lb./sq.in.)

Component	Moles feed	Moles Hydrocarbon rich liquid	Moles water rich liquid	Moles vapor	K_{HC}
Propane	25	7.93	—	17.07	2.33
n-butane	25	11.55	—	13.45	1.26
n-pentane	30	17.74	—	12.26	0.7483
n-hexane	10	7.03	—	2.97	0.4567
n-octane	20	17.27	—	2.73	0.1714
Water	40	1.44	28.91	9.65	7.26
Total	150	62.96	28.91	58.13	

Predicted water solubility in the hydrocarbon liquid is 0.0229 mole fraction.

various solid phases may form.

Lu et al. (1974) have developed a modified regula-falsi method for calculating three-phase vapor-liquid-liquid equilibria. Lu's modification of the Redlich-Kwong equation was used with different parameters for each component in each of the three phases at equilibrium.

Dluzniewski et al. (1973) have outlined an application of free energy minimization to solve a liquid-liquid-vapor equilibrium problem.

The procedure used here is also based on free energy minimization. In detail it is much different from the procedures of Dluzniewski et al., Erbar, or Lu et al. It is presented in the Appendix.

EXAMPLES

Two numerical examples of three-phase equilibrium results will be presented. The first deals with the same hypothetical mixture used as an example by Erbar (1973). The second deals with the system methane, *n*-butane, water and those results are compared with the experimental data of McKetta and Katz (1948).

Water, Paraffin Mixture

Three-phase flash computations were performed on a system made up from 25 moles of propane, 25 moles of *n*-butane, 30 moles of pentane, 10 moles of *n*-hexane, 20 moles of *n*-octane, and 40 moles of water. With the pressure held at 23.8 atm (350 lb./sq.in.), the number of moles in each of the three phases and the phase compositions were computed over a range of temperatures. The results of these calculations are presented in Figure 4 along with the condensation curves presented by Erbar (1973) for this mixture.

Erbar's condensation curves and the condensation curves from this work are strikingly similar. The major difference is that Erbar's predicted bubble point and dew points are 3 to 5°K lower than those computed here. In Erbar's calculations a separate description is used for each phase. In this work, all three phases are described by Wilson's version of the Redlich-Kwong equation.

The detailed results of computations at 422°K (300°F) are summarized in Table 4. These results also are very similar to those of Erbar. The major difference is that in this work the mole fraction of water in the hydrocarbon liquid is 0.0229 and in Erbar's procedure it is calculated to be 0.0075. Procedure 9A1.5 in the API Technical Data Book predicts a water solubility of 0.036 mole fraction. If the hydrocarbon-water interaction parameters were increased, a higher water solubility would be predicted. Values of $k_{ij} = 0.50$ were employed here.

Methane, *n*-Butane, Water

Phase equilibrium computations were performed on the system methane, *n*-butane, water which has been studied experimentally by McKetta and Katz (1948). The interaction parameter for the methane, *n*-butane pair was fixed at $k_{12} = 1.01$. This value was selected to match the binary vapor liquid equilibrium data at 311°K (100°F) and 20.4 atm (300 lb./sq.in.). The *n*-butane, water interaction parameter was set at 0.50 as in the preceding calculations. Although the methane, water interaction parameter could have been manipulated to match some of the three-phase data of McKetta and Katz it was found unnecessary to do so since a value of 0.50 provided a very good match of the water mole fraction in both the hydrocarbon rich phase and the vapor phase at 311°K.

The methane, *n*-butane vapor liquid equilibrium results are presented in Figure 5. Calculated results are presented for the binary two-phase data and for the ternary three-phase data. In both cases there are two degrees of freedom and the temperature and pressure fix the composition of all three phases. In the case of the ternary data the compositions of the vapor and hydrocarbon liquid phases are reported on a water free basis.

One of the more interesting features of the McKetta and Katz data is that the presence of water has a large effect on the hydrocarbon vapor liquid equilibrium in some ranges of temperature and pressure. At 344°K (160°F) and 378°K (220°F) it was found experimentally that the water saturated vapor was relatively more rich in methane than the dry vapor.

In the calculated equilibria, the presence of water proves to be important only at temperatures higher than 378°K. The computed water saturated vapor is relatively less rich in methane than the computed dry vapor.

The data of McKetta and Katz include the three-phase critical region. They found that the three-phase critical pressure at a given temperature was consistently slightly higher than the methane, *n*-butane critical pressure at the same temperature.

Although the calculation scheme employed is not suitable for locating critical points exactly, it was possible to

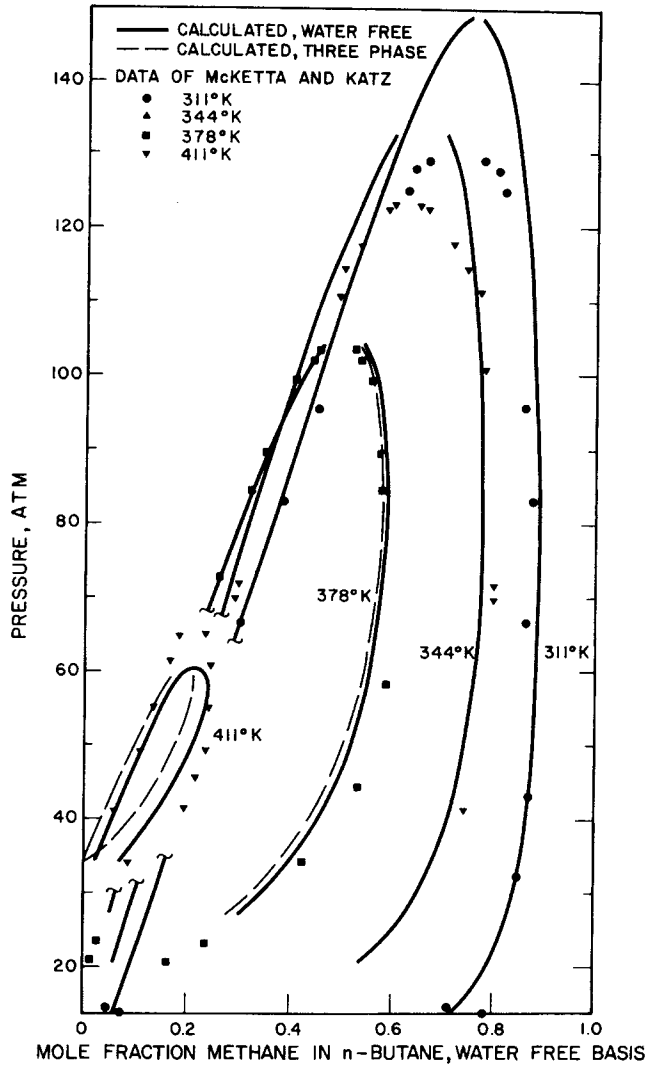

Fig. 5. Vapor-liquid equilibrium in the system methane, *n*-butane water.

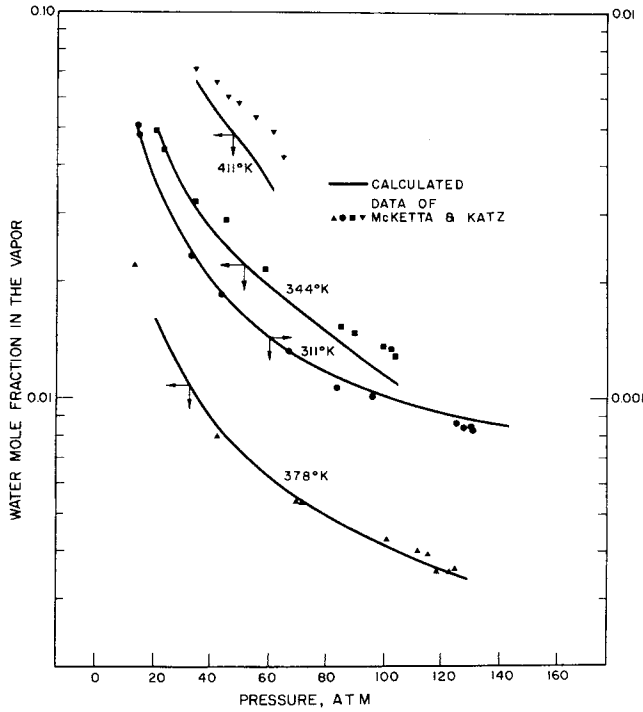

Fig. 6. Water mole fraction in the vapor phase; three-phase equilibria in the system methane, *n*-butane, water.

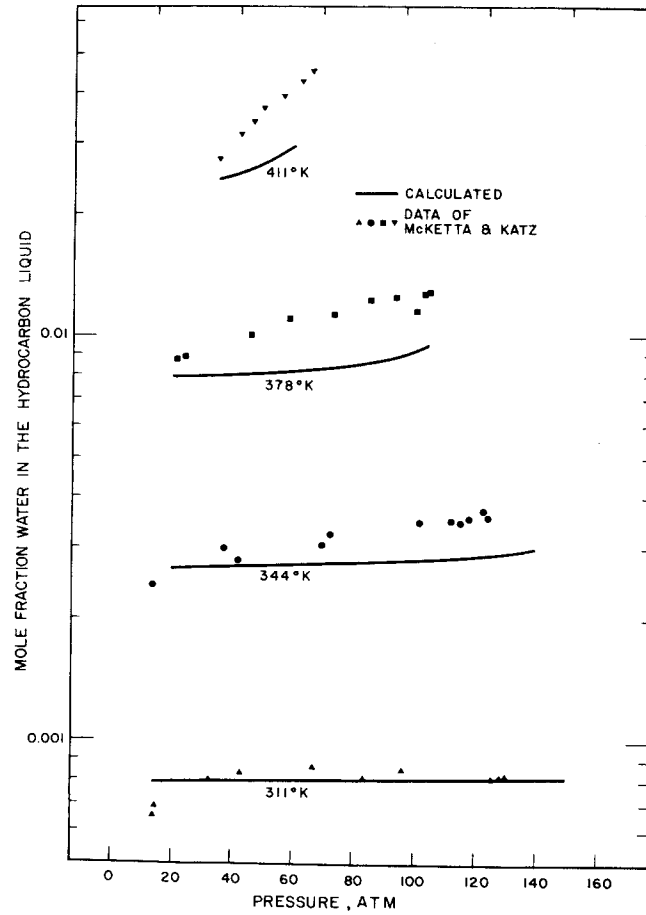

Fig. 7. Water mole fraction in the hydrocarbon liquid; three-phase equilibria in the system methane, *n*-butane, water.

complete computations close to the two-phase and three-phase critical points. The qualitative behavior of the three-phase critical pressure given by Wilson's version of the Redlich-Kwong equation is consistent with the experimental data in being slightly higher than the computed binary critical point at a given temperature.

The agreement with experimental critical data is variable. At low temperatures, calculated critical pressures are high, at 378°K the agreement is very good, and at higher temperatures the calculated critical pressure is too low.

The water content of the two hydrocarbon phases in the three-phase region is presented in Figures 6 and 7. The calculated water mole fraction in the vapor phase agrees extraordinarily well with the experimental data at 311° and 344°K but is low at the higher temperatures. This agreement can, no doubt, be attributed to the success of Wilson's version of the Redlich-Kwong equation at matching the vapor pressure of pure substances and at describing the vapor phase. Since the water phase is almost pure water, the vapor pressure of water plays a large role in determining the water content of the vapor phase.

The computed water mole fraction in the hydrocarbon liquid, as can be seen in Figure 7, is in agreement with the experimental data at 311°K and is somewhat low at higher temperatures. The agreement is comparable to that obtained for pure *n*-butane. The match between the experimental data and computed results could be improved by making the water, hydrocarbon interaction parameter an increasing function of temperature. Nonetheless, the calculated mole fractions are no more than 30% low over the whole of the experimental range and at the lower pres-

Table 5. High Pressure Solubility of Water in Methane, *n*-butane

	Mole fraction CH_4, water free	Mole fraction water			
		$P = 136.1$ atm		$P = 204.1$ atm	
T°K		Calc.	Exptal.	Calc.	Exptal.
311	0.732	0.000849	0.000804	0.000745	0.00065
344	0.630	0.00303	0.00328	0.00251	0.00274
378	0.4925	0.00832	0.01056	0.00661	0.00795
411	0.219	0.01640	0.0253	0.01330	0.0193

sures the agreement is considerably better.

The instability of the liquid phase continues at pressures above the three-phase critical pressure for the mixture. It has been possible to calculate the water mole fraction in the hydrocarbon liquid at 136.1 atm (2000 lb./sq.in.) and 204.1 atm (3000 lb./sq.in.) and compare these results with experimental data. The composition of the hydrocarbon liquid has been taken to be the composition at the three-phase critical at the given temperature. The calculated and experimental results are presented together in Table 5.

Quantitative agreement of the calculated results with the experimental results is better at lower temperatures. As before, the agreement at higher temperatures could be improved by making the interaction parameters an increasing temperature function. Perhaps more interesting is that the qualitative effects of pressure on the water solubility in the hydrocarbon phase are duplicated by Wilson's version of the Redlich-Kwong equation. In both the experimental and computed results, the equilibrium water content decreases as pressure is decreased, following the trend which exists at pressures below the three phase critical point in the vapor phase. Up to the three-phase critical pressure the water content of the hydrocarbon liquid is seen to increase as pressure is increased.

The hydrocarbon content of the water rich liquid is, of course, not accurately predicted at any temperature or pressure. It was possible to select k_{12} to match equilibrium data in one of the liquid phases but not in both and, as stated before, it was decided to concentrate on the hydrocarbon liquid. If accurate predictions of hydrocarbon mole fractions in the water liquid are required, some other procedure must be used.

However, in some respects the behavior of the computed results does correspond qualitatively with the experimental data. The methane solubility is computed to increase sharply with pressure while the *n*-butane solubility decreases. At 378°K, the computed methane mole fraction varies from 0.396×10^{-6} to 1×10^{-5} as pressure varies from 20.4 to 103.4 atm. The corresponding experimental values are 0.5×10^{-4} and 1.30×10^{-3}, respectively. On the other hand, the computed *n*-butane solubility decreases slightly from 0.576×10^{-10} to 0.422×10^{-10} over the same pressure range. At 378°K, experimental data are 0.286×10^{-3} and 0.98×10^{-4} for the mole fraction of *n*-butane in the water phase at 20.4 atm and 103.4 atm, respectively.

In the experimental data, the total hydrocarbon solubility in the water phase is shown to pass through a minimum as temperature increases at constant pressure. This important qualitative result is not in any way apparent in the computed equilibrium solubilities. At every pressure, the computed mole fraction of the total hydrocarbons in the water phase increases exponentially with temperature.

SUMMARY OF EXAMPLES

The three-phase hydrocarbon water equilibrium examples discussed here demonstrate that it is feasible to describe all three phases by a single equation of state. Although the Wilson version of the Redlich-Kwong equation was used here, the same approach is likely to yield similar results with other equations of state.

Many of the important qualitative characteristics of these three-phase systems are correctly predicted in this approach. The quantitative agreement between the calculated and experimental values of the water content in the two hydrocarbon phases is sufficiently good to consider the use of the proposed procedures for design purposes.

NOTATION

a, b = parameters in the Redlich-Kwong equation
a_{ij} = coefficient defined by Equation (5)
b_i = coefficient defined by Equation (4)
f = fugacity
G' = defined by Equation (A.18)
k_{ij} = interaction parameter for the i, j pair
n, p, q, r = mole numbers
P = pressure
P_c = critical pressure
R = universal gas constant
T = temperature
T_c = critical temperature
V = molar volume
x = mole fraction
Z = compressibility factor

Greek Letters

ΔG^M = standard Gibbs free energy of mixing
ω = acentric factor

Subscripts

i, j, k = substance index
I, II, III = phase index

LITERATURE CITED

API Technical Data Book, American Petroleum Inst., Div. of Refining, Washington, D. C. (1970).

Deam, J. R., and R. N. Maddox, "How to Figure Three-Phase Flash," *Hydrocarbon Proc.*, 78(7), 163 (1969).

Dluzniewski, J. H., S. B. Adler, H. Ozkardesh, and H. E. Barner, "Aid to Correlation of Complex Equilibria," paper presented at the 75th National AIChE Meeting, Detroit (1973).

Erbar, J. H., "Three Phase Equilibrium Calculations," *Proc. 52nd Ann. National Gas Processors Assoc. Meeting*, 62 (1973).

Kohn, J. P., "Heterogeneous Phase and Volumetric Behavior of the Methane *n*-Heptane System at Low Temperatures," *AIChE J.*, 7, 514 (1961).

Lu, B. C.-Y., P. Yu, and A. H. Sugie, "Prediction of Vapor-Liquid-Liquid Equilibria By Means of a Modified Regula-Falsi Method," *Chem. Eng. Sci.*, 29, 321 (1974).

McKetta, J. J., Jr., and D. L. Katz, "Methane-*n*-Butane-Water System in Two-and Three-Phase Regions," *Ind. Eng. Chem.*, 40, 853 (1948).

Prausnitz, J. M., "Molecular Thermodynamics of Fluid-Phase Equilibria," Prentice-Hall, Englewood Cliffs, N. J. (1969).

Schindler, D. L., G. W. Swift, and F. Kurata, "More Low Temperature V-L Design Data," *Hydrocarbon Proc.*, 45 (11), 205 (1966).

Wilson, G. M., "Vapor-Liquid Equilibria, Correlation by Means of a Modified Redlich-Kwong Equation of State," *Adv. Cryogenic Eng.*, 9, 168 (1964).

———, "A Modified Redlich-Kwong Equation of State, Application to General Physical Data Calculations," paper presented at the 65th National AIChE Mtg, Cleveland (1969).

APPENDIX A. THREE-PHASE FLASH CALCULATION PROCEDURE

The following development is applicable to flash type calculations only. While extensions of the approach taken here to dew point or bubble point calculations may be possible, there are some conceptual difficulties.

A given mixture consisting of $n_1, n_2, \ldots, n_N$ moles of the respective substances is postulated to separate into three phases having $p_1, \ldots, p_N$ moles in phase *I*, $q_1, \ldots, q_N$ moles in phase *II*, and $r_1, \ldots, r_N$ moles in phase *III*. Conservation of mass requires that

$$p_i + q_i + r_i = n_i \tag{A.1}$$

and all the mole numbers must, of course, be nonnegative. Given these constraints, the system must split into three phases at the given temperature and pressure in such a way that the Gibbs free energy is minimized.

There are two independent mole numbers for each substance in the problem as stated and it is desirable to leave some flexibility for a given substance, say substance i, in selecting p_i, q_i or p_i, r_i or q_i, r_i as the independent pair. Whichever pair is chosen as independent, it is quite a simple matter to form the gradient of the Gibbs free energy. Taking p_i and q_i as independent

$$\frac{\partial G/RT}{\partial r_i} = \ln f_{iI} - \ln f_{iIII} \tag{A.2}$$

$$\frac{\partial G/RT}{\partial q_i} = \ln f_{iII} - \ln f_{iIII} \tag{A.3}$$

Taking p_i and r_i as independent

$$\frac{\partial G/RT}{\partial p_i} = \ln f_{iI} - \ln f_{iII} \tag{A.4}$$

$$\frac{\partial G/RT}{\partial r_i} = \ln f_{iIII} - \ln f_{iII} \tag{A.5}$$

Taking q_i and r_i as independent

$$\frac{\partial G/RT}{\partial q_i} = \ln f_{iII} - \ln f_{iI} \tag{A.6}$$

$$\frac{\partial G/RT}{\partial r_i} = \ln f_{iIII} - \ln f_{iI} \tag{A.7}$$

For different substances different choices may be made about the independent mole numbers.

Supposing that p_i and q_i are independent, the path of steepest descent in the free energy, from any initial condition, is given by

$$\frac{dp_i}{dt} = -\ln f_{iI} + \ln f_{iIII} \tag{A.8}$$

$$\frac{dq_i}{dt} = -\ln f_{iII} + \ln f_{iIII} \tag{A.9}$$

where t is a dummy variable. It appears that Equations (A.8) and (A.9), (or similar equations) can be integrated to reach the point of minimum free energy, at which point $dp_i/dt = 0$ and $dq_i/dt = 0$ and equality of fugacities is assured. There is, however, the possibility that one of the phases must disappear at equilibrium so that there is no equilibrium point which corresponds to nonnegative mole numbers.

On the other hand, the following equations also move toward the minimum Gibbs free energy but the solution is limited to nonnegative p_i and q_i.

$$\frac{dp_i}{dt} = -p_i \ln(f_{iI}/f_{iIII}) \tag{A.10}$$

$$\frac{dq_i}{dt} = -q_i \ln(f_{iII}/f_{iIII}) \tag{A.11}$$

In integrating these (or similar) equations, accuracy of the integration is not important. It is only important to approach the stationary state as rapidly as possible. These considerations motivate the use of an integration procedure which is simple but which permits use of a relatively large increment Δt.

In this work the integration of Equations (A.10) and (A.11) is approximated by

$$p_i^{j+1} = p_i^j (f_{iIII}/f_{iI})^{\Delta t} \tag{A.12}$$

and

$$q_i^{j+1} = q_i^j (f_{iIII}/f_{iII})^{\Delta t} \tag{A.13}$$

where p_i^{j+1} and p_i^j are trial values of the mole number p_i at successive steps of the integration or in successive iterations. These formulas are virtually Euler's forward integration of the differential equations.

It is possible to assure that negative mole numbers can never be generated by using Equations (A.12) and (A.13) only if $f_{iIII} < f_{iI}$ and $f_{iIII} < f_{iII}$; that is, only if both p_i and q_i are decreasing. Otherwise, if $f_{iI} < f_{iII}$ and $f_{iI} < f_{iIII}$ then equations

$$q_i^{j+1} = q_i^j (f_{iI}/f_{iII})^{\Delta t} \tag{A.14}$$

and

$$r_i^{j+1} = r_i^j (f_{iI}/f_{iIII})^{\Delta t} \tag{A.15}$$

are used. If $f_{iII} < f_{iI}$ and $f_{iII} < f_{iIII}$, then equations

$$p_i^{j+1} = p_i^j (f_{iII}/f_{iI})^{\Delta t} \tag{A.16}$$

and

$$r_i^{j+1} = r_i^j (f_{iII}/f_{iIII})^{\Delta t} \tag{A.17}$$

are used. With these equations the mole numbers being iterated upon are certain to be decreasing. The remaining mole number is calculated from Equation (A.1) and cannot become negative.

It remains to find the increment Δt in this procedure. The criterion that must be met is that at each stage of the computation the total Gibbs free energy of the system decreases. It is possible to show that, in the vicinity of the minimum point, there is a maximum Δt for which the free energy decreases and that this Δt is also the maximum increment for Euler's forward integration to be stable. Furthermore, this maximum Δt is a constant and convergence is assured if any value less than this constant value is used in the iterations.

The iterative procedure which was used involves determining at each step whether the free energy of the system has decreased. It is equivalent that G' decrease where

$$G' \equiv \sum_i (p_i \ln f_{iI} + q_i \ln f_{iII} + r_i \ln f_{iIII}) \tag{A.18}$$

The quantity G' is simple to compute from quantities which must be computed at each iteration in any case. If G' has in fact decreased, Δt is increased,

$$\Delta t^{j+1} = 1.1\ \Delta t^j \tag{A.19}$$

If at some stage G' is found to increase, then Δt is decreased

$$\Delta t^{j+1} = 0.7\ \Delta t^j \tag{A.20}$$

It has been found necessary to prevent Δt from ever again increasing after having once been decreased so that oscillations can be avoided. The factors 1.1 and 0.7 in Equations (A.19) and (A.20) are arbitrary but appear to be satisfactory.

It has also been found desirable to start iterations with a small Δt, say $\Delta t = 0.02$, so that in the initial part, the process closely approximates integration and large changes in the mole numbers can be avoided.

The speed of convergence of this procedure depends on the proximity of the equilibrium condition to any critical points and, to a large extent, on the composition of the mixture being flashed. Convergence is slow, in general, when the quantity of one of the phases becomes small at equilibrium.

It has been observed also that near the dew point or bubble point conditions it is possible to converge to an incorrect solution in which there is only one hydrocarbon phase, depending on the initial guess of the phase compositions.

Since for each component of the mixture there are three different possible sets of equations to be used in the computations, there are $3N$ permutations in the overall set of equations. The convergence properties are variable depending on exactly which set of equations is used.

Convergence depends to some extent on the scheme used to obtain the increment Δt. Equations (A.19) and (A.20) were

used in this study, but it is obvious that other procedures could be employed.

The convergence criterion used was that

$$\sum_i [|\ln f_{iI}/f_{iIII}| + |\ln(f_{iII}/f_{iIII})|] < 1 \times 10^{-4}$$

With this criterion, convergence occurred, at best, with 50 iterations. At worst more than 1000 iterations may be required.

Computations were performed on a CDC 6400. On this machine the computing time was roughly 0.003 sec./iteration per component. As indicated, computing time increases linearly with the number of components.

The advantages of this procedure lie in its ease of formulation and programming, its tie to thermodynamic principles, and its reliability. The formulation presented here can easily be extended to more than three phases which makes it a candidate for use in computations where solid phases need be considered, as in cryogenic applications.

Since the procedure minimizes free energy, it is possible to avoid spurious solutions to the equilibrium problem such as those pointed out in the discussion of Figure 5e. In the liquid-liquid-vapor computations the starting point was that almost all the water was in a water rich liquid with a few percent of the total water being present in the two hydrocarbon rich phases. The hydrocarbons were distributed so that the vapor phase was rich in the light components and the liquid phase was rich in the heavy components. This assured convergence to the correct equilibrium conditions.

Manuscript received January 31, 1974; revision received May 16 and May 20, 1974.

Determination of the Kinetics of Secondary Nucleation in Batch Crystallizers

The kinetics of secondary nucleation have been determined from measurement of the supersaturation as a function of time following the addition of seed nuclei to a supercooled solution in a well-stirred batch crystallizer. Population balance mathematics have been used to show that the secondary nucleation kinetics may be inferred from the supersaturation-time curve. The method has been applied to the determination of the kinetics of the secondary nucleation of ice and found to give results in excellent agreement with those obtained from tedious particle counts. In addition, it has been shown that the moment of the particle size distribution that best correlates the nucleation rate data can be inferred from the initial transient of the supersaturation-time history.

S. G. KANE
T. W. EVANS
P. L. T. BRIAN
and
A. F. SAROFIM

Department of Chemical Engineering
Massachusetts Institute of Technology
Cambridge, Massachusetts 02139

SCOPE

The use of batch crystallizers for the determination of the kinetics of secondary nucleation is complicated by the variation during an experiment in both the number of crystals and the supersaturation. Motivation for the use of batch crystallizers is provided, however, by the relative ease with which a large range of operational variables may be studied in a short time.

This paper develops techniques for obtaining kinetics of secondary nucleation for one mode of operation of a batch crystallizer. A seed crystal is introduced in a supercooled solution and measurements are made of the variation with time of either the number of crystals or the supersaturation. Up to a critical time, designated here as the induction time, the multiplication in the number of crystals occurs with an insignificant variation in the supersaturation. Measurement of the number of crystals during his period of relatively constant supersaturation provides one method of obtaining nucleation kinetics. Particle counts, however, may be tedious or difficult, particularly for systems such as ice where crystals are relatively unstable. One major objective in this paper is therefore the development of methods for inferring nucleation kinetics from the supersaturation measured at times greater than the induction time.

It should be noted that the inference of nucleation kinetics is complicated by the fact that the rate of secondary nucleation may be proportional to the nth moment of the particle size distribution

$$\dot{N} = a_n \mu_n$$

Complete characterization of the nucleation kinetics would therefore require the determination of two parameters n and a_n. It will be shown, however, that a single

Correspondence concerning this paper should be addressed to A. F. Sarofim. S. G. Kane is with Amoco Chemicals Corporation, Naperville, Illinois. T. W. Evans is with The Upjohn Company, Kalamazoo, Michigan. P. L. T. Brian is with Air Products Corporation, Allentown, Pennsylvania.